

Supporting Information

Dewar et al. 10.1073/pnas.1306100110

SI Text S1: 2007–2008 Excavations at the Rock Shelter of Ambohiposa (by H.T.W., R.E.D., and C.R.)

Geology. The Vohémar area flanks the ancient Precambrian continental fragment transferred into granites, migmatites, and other rocks during the Paleozoic and Mesozoic eras. The higher ridges visible today are primarily granite, but other rocks and minerals occur. Of importance to the early human inhabitants was chlorite schist, which was worked into vessels and exported (1). There are also extrusive basalts and sedimentary gravels in which silicates useful for stone tools may be found. Iron oxide nodules, found today eroding from iron-rich ultisols in and near marshes, may have been the source of iron ore used by early blacksmiths.

The coastal areas manifest a complex development of Pleistocene and Holocene shoreline features. The active beach extends up to 2 m above high tide, and has evidence of modern occupation. The second and third beaches, from 2 to 4 m above high tide, have weakly developed soils and evidence of occupation during the past millennium. Higher beaches with deeply developed red soils, well above the level of the rock shelter reported here, are not yet well dated (2, 3).

Climate. Vohémar is located along a climatic gradient from the more arid and seasonal extreme north to the more humid east coast. The mean annual rainfall is 1,413 mm, with January having the highest mean, 203 mm, with the least rainfall in September (55 mm). Vohémar has a tropical climate with relatively little annual variation in temperature: its warmest month is January (mean daily maximum of 31.2 °C) and coolest month is August (27.3 °C).

As in many areas of Madagascar, there is a very high frequency of tropical cyclones with damaging winds and floods. Between 1960 and 1974 Vohémar was struck by cyclones six times (4). The coastline is directly exposed to the southeastern trade winds of the austral winter, and sea conditions in those months are often dangerous for small craft. However, the harbor of Vohémar, protected by its massive reef and sand bank, is as well protected as any on the east coast of Madagascar.

Flora and Fauna. Today this region is covered with a mosaic of grassy pasturelands, dry and humid forest remnants, brushy secondary growth, dry fields on slopes, irrigated rice fields on valley bottoms, wetlands, and close to the coast significant areas of plantations of coconut (*Cocos nucifera*). There are small areas of surviving coastal forest, such as that as at Sahaka, about 30 km north of Vohémar. The forest is a littoral remnant of Western Dry Forest with an emergent canopy 10–15 m in height, dominated by trees of the Anacardiaceae, Pandanaceae, Rubiaceae, and Sapindaceae (5). There are five species of lemurs (*Microcebus rufus*, *Lepilemur* sp., *Eulemur coronatus*, *Propithecus tattersalli*, and *Cheirogaleus* sp.) (6), three species of tenrecs, including the often hunted *Tenrec ecaudatus*, the introduced rodent *Rattus rattus* (7), and two species of bats, including the often hunted *Pteropus rufus* (8). There is only one larger terrestrial mammal, the bushpig, *Potamochoerus larvatus*, possibly introduced from East Africa. In the past, there were almost certainly other larger species that early human occupants could have hunted, including large flightless birds, the pygmy hippopotamus, and various larger lemurs, but apart from ratite eggshells there is no fossil evidence.

Excavations at Ambohiposa. The rockshelter of Ambohiposa is situated in the east-facing slope of a massif of Mesozoic igneous and sedimentary rocks, including layers of basalt, marl, siltstone, and sandstone, reaching altitude of 80 m. The shelter is one of several at the base of an outcrop, about 50 m above sea level, and has a good view northeast over the Bay of Iharana and the low plain to its south composed of sand ridges separated by marshy areas. The sheltered area of Ambohiposa is small, only 4 m from north-northwest to south-southeast (Fig. S1). Today the overhang protects only about 1.2 m from the back wall to the drip line, but blocks of stone down the slope may be parts of a larger overhang, now collapsed. In brief, the shelter could not house a large group and was probably used by only a few foragers for protection from downpours or for an overnight camp.

In 2007, we placed a small rectangular excavation extending 130 cm from the back of the shelter to the drip line and 50 cm in width. In 2008, we placed two parallel 0.50 by 1.00+ m units, one 0.50 m to the north and one 0.50 m to the south of the first season's unit. The northern unit had a thin and compressed organic layer. At first we thought this was the upper organic layer from the previous year's unit, but we continued down below the level of the deepest red silt year of the previous year and realized that the upper organic layer must be layers 3–5 compressed together. The southern unit was similar to the initial unit, but had thicker and better-defined organic layers. These layers were unfortunately somewhat disturbed close to the back wall of the shelter, probably by rodents. This report presents a synthetic stratigraphy for the central and northern units (Table S1). Within each unit, different layers had slightly different volumes because the back of the shelter was irregular and some layers contained large rocks, the approximate volumes of which were subtracted from the volume excavated to better approximate the volume screened. The deposits were excavated in six natural stratigraphic layers as follows, with estimates of average thickness:

Layer 1 (0.03 m): Brownish silt, angular rock fragments and recent leaf litter;

Layer 2 (0.10 m): Brown silt and angular rock fragments (Munsell 7.5YR 4/3);

Layer 3 (0.11 m): Very dark grayish brown fine silt with a few small stones (Munsell 10YR 3/2);

Layer 4 (0.15 m): Brown silt with many angular or flat rock fragments (Munsell not taken);

Layer 5 (0.05 m): Very dark grayish brown silt with few small rock fragments (Munsell 10YR 3/2);

Layer 6 upper (0.04 m): Dark brown silt with rounded pebbles (Munsell 7.5YR 3/4);

Layer 6 lower (0.05+ m): Dark brown silt with angular rock fragments (Munsell 7.5YR 3/4).

Sediment samples from Ambohiposa have been studied by Paul Goldberg and F.B. at Boston University. They have established that a major component of silty material found in all levels is kaolinite, which is forming on the hilltop above and could have been washed over the cliff. A minor component is quartz, which could have been a component of the bedrock or introduced by wind or water (Text S6). We suggest the following depositional history. A period of weathering and the deposition of strongly oxidized kaolinitic sediment ends with the deposition of layer 6. Organic layer 5 formed on the surface and is the surface on which

one or more brief occupations by people using stone tools. A probably brief period of spalling of the back wall or roof leads to the deposition of layer 4, largely a deposit of stone debris. This layer is succeeded the further deposition of organic material, with possible evidence of further occupations by people creating layer 3. These organic sediments are sealed under layer 2, a thin layer of oxidized reddish sediment, probably washed from above relatively recently. Layer 1 is the layer of recent leaf litter.

Each context was excavated with trowels and sieved in a 3-mm screen. The larger natural rocks were examined for evidence of use and then discarded. Possible chert, bone, and charcoal fragments were saved, and everything remaining was carried to Vohémar to be washed through 1-mm screen in the sea, dried, and sorted under magnification. We excavated ~25% of the area of layers 3–5.

Flaked Stone Assemblage from Ambohiposa. Flaked stone items recovered primarily from our washing and sorting procedure were very small; a majority from a range of crypto-crystalline silicates which we term “chert” and a minority of a volcanic glass which we term “obsidian.” The chert items can be opaque and gray, tan or brown, or translucent and brown in color. The few unmodified pieces are less than 2 cm in length. Included are rare flakes of a translucent agate, white or gray in color. Some of the fragments and flakes have glossy surfaces and pot-lid flakes attributable to either deliberate heating to improve flaking qualities or to accidental burning. The obsidian is usually opaque and black. Tiny pieces of brown chert were found in coarse igneous rock that forms the outcrop. Survey in the area of Ambohiposa identified small blocky fragments of opaque brown chert in a gully 80 m north of the shelter and small rounded pebbles of translucent gray and white agate on the slope of the hill of Ambatomalana 180 m to the northwest of the shelter. We found few definite pieces of this agate in our flaked stone assemblage. We have found only one published record of volcanic glass from Madagascar, 400 km south-southwest of Vohémar (9).

Some Ambohiposa flaked chert items probably result from direct percussion on small amorphous flake cores. Other items, however, result from a simple and widely known reduction procedure termed “smash-and-select” or “bipolar reduction” (10–12) used throughout the world wherever available raw material pieces are small. In such cases it is difficult to control the platform, the striking angle, and other variables that allow a flint knapper to produce piece of the right size for tools. The small piece of raw material was placed on a large rock or “anvil” and struck with a smaller rock or “hammer stone.” Both the flakes and the remnant core have flake scars that originate from both the hammer blow and the large stone below. Flakes of useful size and shape were selected, used as is, or modified for specialized use. The larger remnant pieces of raw material struck again and the selection procedure repeated again until only small pieces of shatter remained. In our three units, there are no larger chert flake cores or recognizable fragments of such cores. There is, however, a bipolar core remnant of chert (Fig. 2A) with scars on both faces originated from both ends and a few small fragments of such cores.

Chert waste recovered by our fine-screen washing procedure includes 2002 pieces of blocky shattered chert weighing a total of 189 g. Some of the shatter fragments—many of which are very small, particularly of the brown chert that occurs not far from Ambohiposa—could be a product of natural fracture. It is the flakes that have the most interesting implications for past human activity. We recovered 292 flakes—thinner pieces of chert with an exterior face with the scars left by earlier flake removals and an inner face resulting from their removal from the core—weighing a total of only 14 g. Most of these are not weathered and exhibit bulbs from directed percussion or pressure.

Some of the larger flakes are products of bipolar core reduction. One flake (Fig. 2B) has scars on both faces originated from both ends. This sample was used on one edge, as indicated by very small flakes along one edge, but not otherwise reworked or broken. Others are probably fragments of such flakes. Two modified items are made from crescent-shaped pieces of opaque tan chert, triangular in cross-section, probably resulting from bipolar reduction. Both items are from the older reddish sediment of layer 6 in the north unit are thus possibly older than the other items discussed here. Both have slight overall light polish and possible manganese accretions, probably of geological origin, which makes it difficult to interpret to sequence and direction of flake removals. The larger (Fig. 2C) is made from the distal fragment of a large flake used for bipolar work. Small blade-like flake scars originate at either end of the item, and there are a few small retouch flakes narrowing the two ends. The smaller flake (Fig. 2D) has removal scars only from one end, and thus is not formally bipolar. The flake is not systematically retouched, but has a number of small edge removals that emphasize its crescentic shape. Note that neither of these are typologically “crescents” because they are made from bipolar flakes not blade segments and are not backed.

Some flakes do not have clear evidence of flakes struck from two ends and may have been detached from larger blocky or amorphous cores by a direct blow of the hammer stone without an underlying anvil. One nearly complete brown chert flake appears to be a product of conventional flake removal from such a core (Fig. 2E). The outer surface was guided by a previous flake removal on the left and secondary retouch flakes struck from the right. The inner surface shows that the platform was removed by small secondary flakes and a pot-lid. Nibbling on the edges could result from binding to a haft and polish on the tip suggests use in cutting or perforating.

Fragments of larger flakes without clear evidence of flakes struck from two directions may have been detached from either bipolar cores or larger blocky or amorphous cores. A brown chert flake (Fig. 2F) has small flakes removed from its left edge, perhaps from utilization or perhaps from retouch to create a reinforced edge useful in scraping. One similar flake, not illustrated, has a small notch made with multiple secondary removals. Two chert flake fragments are notable for their trapezoidal shape. One fragment (Fig. 2G) is probably the proximal end of a larger flake struck from the weathered surface of a tan chert pebble. The left side of this flake was retouched to emphasize the trapezoidal shape. The other fragment (Fig. 2H) is from the distal end of a translucent brown flake, otherwise represented by two tiny retouch flakes, ending on the weathered surface of a fragment. The upper surface is formed by flakes converging from either side of this flake, and the piece was detached from the proximal end of the original flake by a blow on the ridge where they meet. No additional retouch was needed to create a trapezoidal form. We emphasize that neither of these fragments are typologically “trapezes” because they are not made from blade segments by retouching or backing both the distal and proximal sides.

Finally, there are a few small narrow parallel-sided chert flakes that may be termed microblades. One chert example (Fig. 2I) is complete, and the scars on the anterior face show that it was one of a series pressed from a core similar to the obsidian core noted below. Retouch is uncertain. Another medial segment of chert (Fig. 2J) does not have the characteristic parallel scarring on the anterior face, and may be simply an accidental flake from the edge of a small blocky core of chert. Such parallel-sided flakes are often created in shaping a blocky piece into a core, and are not true blades.

Obsidian waste recovered by the fine-screen washing procedure includes one obsidian microblade core fragment weighing 0.17 g and 18 tiny obsidian flake and microblade fragments weighing 0.52 g. The fragment of a microblade core of obsidian (Fig. 2M)

has the scars of three microblade removals. The widest of these removals is 0.38 cm. Retouch from the right side could result from use of the core as a scraper after it was exhausted. An obsidian flake may have utilization on its pointed right side (Fig. 2L). A microblade medial segment of obsidian (Fig. 2K) is 0.35 cm wide has possible retouch on the left edge. This segment could have been removed from a core similar to the one represented by the fragment described above.

It must be emphasized that this is a small sample of tiny items. Backed microblades, retouched points, or multiply notched tools that would be convincing to all stone tool specialists are not present. Nevertheless, the fact that most of the raw materials do not appear to occur in the rock shelter and must have been carried in, the evidence of directed blows detaching a series of flakes from cores, and the evidence of retouch or use on some pieces indicate that this is a stone tool industry created by people.

The distributions of the densities and size of stone items in layers 3–6 (Table S1) provide additional evidence of the conditions under which they were deposited:

Coarse flakes of the rhyolite, which forms the back wall of the rock shelter are most plausibly interpreted—given the scarcity of bulbs of percussion and the absence larger artifacts, such as chopping tools or heavy scrapers from which they might have been struck—as natural consequences and an index of weathering of the shelter wall and overhang.

Chert shatter is interpreted as primarily a by-product of bipolar core working. Shatter is most common and larger in contexts in layers 4 and 5. Examples in upper layer 3 are few and small and may be extrusive from lower layers, but there is a possibility of continuing ephemeral occupation. Examples in the uppermost part of layer 6 are common but small. Shatter has perhaps been carried down into layer 6 by physical disturbance.

Both chert flakes and volcanic glass flakes are interpreted as the products of core-working or by-products of retouching larger flakes such as scrapers. By density, both chert and volcanic glass flakes are most common in layer 5. Obsidian flakes are rare, but present in layer 3 and upper layer 6. Chert flakes are relatively common from layers 3–5. The flakes in layer 6 may have been carried down by physical disturbance.

The other items, including core fragments, possible tools made on flakes, microblades and microblade segments, which are individually illustrated and discussed above, are scattered throughout layers 2–6, but concentrated in layers 3–5.

We note that the strong proportion of shatter is typical of samples from stone tool-making loci that have been washed through very fine screens. To our experience with sites elsewhere in the world, this is a low density of possibly cultural stone debris, what one would expect from brief visits and limited manufacture or resharpening of tools. If our 25% sample is representative, only about 800 g of raw material would have been discarded at Ambohiposa. The stratigraphic distribution of items indicates that there may have been visits at the time of layers 6–3, but that the strongest evidence for human use of the site was during the time of layer 5.

Other Evidence from Ambohiposa. From layers 3–5 of the north unit, we recovered two very small fragments of pottery, both oxidized to a red color and with very coarse angular quartz inclusions. The inclusions indicate a date during our Ampasimahavelona phase *ca.* A.D. 700–1000 (Beta 267774: 1130 B.P. \pm 40, cal A.D. 888–1025; Beta 267773: 1,180 \pm 40, cal A.D. 780–993), the earliest phase of village occupation near Vohémar, defined from excavations at a site of that name 3 km east of Ambohiposa. Note that in the north unit the upper organic layers are thin and

compressed, and these could be intrusive sherds deposited later than the occupation that left the stone artifacts.

From the light fraction of a 6.0-L flotation sample from the south unit, layer 3, ethnobotanist Amanda Logan (Northwestern University, Evanston, IL) reports three carbonized seeds, probably of the Gramineae or Poaceae.

SI Text S2: 2011 Excavations at the Cave of Lakaton'i Anja (by H.T.W., R.E.D., and C.R.)

Geology. The area around the Baie d'Antsiranana is north of the ancient Precambrian continental fragment metamorphosed into granites, migmatites, and other rocks. This area is underlain by sandy late Mesozoic sediments in which silicates, often re-deposited in gravels, useful for making stone tools, can be found. These sediments were formerly covered by thick marine limestone formations, mainly from reefs of the Eocene and Oligocene Periods. Erosion has reduced these to a few limestone massifs, penetrated by karstic cavities and steep-sided valleys. One of these remnants is the Montagne des Français, southeast of the Baie d'Antsiranana. Extrusive basalts, many flowing from the Montagne d'Ambre, covered and surrounded these earlier geomorphic features in later Tertiary and Pleistocene times. The coastal areas manifest a complex development of Late Pleistocene and Holocene shoreline features (13).

Climate. Antsiranana (formerly Diego-Suarez) has a mean maximum temperature in January of about 31.1 °C and in July of 28.6 °C. The city has mean annual rainfall of 941 mm. The heaviest rains fall in the austral summer months of November through April with a monthly mean total of 271 mm in January, with the least rainfall between May and October with a monthly mean total of 5.2 mm in October (4). This region thus experiences a pronounced dry season, resulting in much of the native local vegetation being largely deciduous.

Discussion of the mean conditions, however, neglects both disastrous natural events, and interannual variability. As in many areas of Madagascar, there is a very high frequency of tropical cyclones with damaging winds and floods in the far north (14); 533 mm has been recorded in a 24-h period (4). In a global comparison of interannual rainfall variability, controlling for mean annual totals, Antsiranana is especially variable (15). In addition, this coastline is directly exposed to the southeastern trade winds of the austral winter leading to dangerous sea conditions. The Baie d'Antsiranana, however, is one of the safest and largest anchorages in the Indian Ocean, although it has only a narrow access to the east, limiting its utility for vessels under sail.

Flora and Fauna. The only paleoecological record of the ecological history of this region comes from a core in the Montagne d'Ambre (16): only the charcoal density in this discontinuous record has been reported, and there is no Holocene record. The paleontological record, however, suggests substantial changes in the late Holocene. Four species of extinct lemurs have been collected in the Montagne des Français: *Pachylemur* sp., *Megaladapis grandidieri*, *Archaeolemur* sp., and *Paleopropithecus maximus*, and three of these (all but *Megaladapis*) were also collected in the Forêt d'Orangea, 10 km to the north. In addition, there are bones of three lemurs no longer locally reported at Andava-koera: *Avahi laniger*, *Propithecus* cf *diadema*, and *Prolemur simus* (17). None of these subfossils have been directly dated, but an *Archaeolemur* from the Ankarana was dated to cal A.D. 988–1177 (18).

Today, the remaining natural vegetation of northern Madagascar is a mosaic of grassy pasturelands, dry forest remnants, humid forests at higher elevations on the Montagne d'Ambre, and with considerable areas of brushy, thorny secondary growth, slope fields, rice pondfields in valley bottoms, tree crops, wetlands, and close to the coast, scattered tracts of coconut (*C. nucifera*).

There are some small areas of coastal Western Dry Forest, usually degraded, with notable levels of biodiversity and endemism. The small Forêt d'Orangea, about 10 km north of the Montagne des Français, is on sandy terrain covering ancient coral reefs, the remnants of high sea stands in Late Pleistocene times (2, 3).

In contrast to these coastal areas is the humid forest on the volcanic massif of Montagne d'Ambre, whose highest peak, 33 km southwest of Montagne des Français, reaches 1,400 m above sea level. A mean annual rainfall of 3,580 mm has been reported from Joffreville (Ambohitra) at about 700 m along the northeast piedmont of Montagne d'Ambre. The forest has an emergent canopy up to 40 m in height. The understory is dominated by palms, tree ferns, and epiphytes. Seven species of lemurs are reported there: *Microcebus arnholdi*, *Cheirogaleus major*, *Lepilemur ankaranensis*, *E. coronatus*, *Eulemur sanfordi*, *Phaner furcifer*, and *Daubentonia madagascariensis*. There are numerous species of Tenrecidae including *Tenrec ecaudatus*, and several species of bats, including the oft-hunted fruit bat (*P. rufus*). Careful survey has recorded 73 species of birds, many endemic, of which the guinea fowl, ibis, herons, and doves are hunted (19, 20).

Intermediate between these drier coastal and more humid montane areas is the karstic plateau of the Montagne des Français. With valley bottoms at 170 m above sea level, and ridges exceeding 350 m, the climate is somewhat more humid and cooler than lower surrounding areas, but no precise measures are available. The ancient Eocene and Oligocene reefs have been deeply affected by solution and in many areas the limestone is composed not of coralline limestone, but of breccias filling karstic cavities. The present rugged topography is a result of the collapse of large cave systems and erosion of the remnant ridges and cliffs by acidic rain, creating sharp spines called *tsingy* ("needles") in Malagasy. These erosional processes leave deep valleys with vertical sides. The vegetation of Montagne des Français—although affected by selective logging, by gardening for papayas, bananas, and manioc, and by cattle grazing—is still impressive. Endemic baobabs (*Adansonia suarezensis* and *Adansonia madagascariensis*) (21), pachypodia (*Pachypodium windsorii*), and succulents (*Aloe suarezensis* and *Euphorbia leuconeura*) (22) dominate the ridges and cliffs. The emergent canopy in the protected valley bottoms and slopes exceeds 30 m. A survey in 2005 and 2006 (23) records diversity of mammals and birds similar to that in the coastal forest remnants. Among the terrestrial mammals, six species of lemurs have recently been observed—*E. coronatus*, *E. sanfordi*, *Microcebus tavaratra*, *L. ankaranensis*, *D. madagascariensis*, and *Cheirogaleus medius*—and another, *Haplemur occidentalis*, is widely reported by local people. Three tenrecs are recorded: (*Microgale* sp., *Setifer setosus* and *T. ecaudatus*). The largest carnivoran of Madagascar, *Cryptoprocta ferox*, is reported by local informants, as are *Galidia elegans* and *Felis silvestris*. Also reported is the African bush pig (*Potamochoerus larvatus*). Domestic cattle (*Bos indicus*) are commonly seen grazing in the valley bottoms. The survey recorded 63 bird taxa, some of which are hunted.

In summary, there is great floristic diversity in the extreme north, but the extant birds and mammals form relatively coherent sets, with sites differing in the number of species reported, but almost always drawn from the same assemblages. Subfossil species identified in the Gorge d'Andavakoera and the Forêt d'Orangea are all also found in the caves of the Ankarana, suggesting that the region's fauna has long been distinctive.

The 2011 Excavation at Lakaton'i Anja. The cave of Lakaton'i Anja is situated on the south side of the Gorge of Andavakoera at the base of a sheer cliff of Eocene coralline limestone. The gorge has vertical cliffs on either side, delimiting a relatively flat floor broken by large fallen blocks and breakdown, which have at times dammed the small stream meandering from west to east,

creating marshy areas. Lakaton'i Anja today looks northeast over a meadow (which was still forested as late as 1990). One climbs from this meadow, southward up a rugged slope of large angular blocks about 6 m to the shelter. The overhang was created by the erosion of a cave, which was parallel to the valley, such that the back wall of the shelter is the south side of the cave. The sheltered sandy floor of Lakaton'i Anja is spacious, 18 m long from east to west, and 4.5 m wide within the drip line. The shelter could easily house a large group of people. Smaller groups could easily have moved around the available space creating a complicated mosaic of overlapping cultural deposits.

The excavations in the 1980s comprised nine 1-m squares, designated with the letters A to I, on a grid oriented north-south/east-west, but the horizontal datum point for this grid is no longer evident. Most of the excavation units of the 1980s work penetrated only the upper layers of the sandy deposit of layer 4. In 2011, we set up a metric grid perpendicular to the rear wall of the sheltered area. This set-up has the advantages of giving us geologically more informative sections transverse to sediment sources outside the shelter and of increasing the probability that we would find the corners, rather than only the sides, of the earlier units. Between July 31 and August 14, we excavated two units, termed J and K. Within each unit, different layers had slightly different volumes because the layers had different thicknesses and some layers contained large rocks and termite disturbances, whose approximate volumes were subtracted from the volume excavated to approximate the volume screened. The deposits from the surface to almost 0.70 m depth below surface were excavated in natural stratigraphic layers with most layers being removed in up to four arbitrary spits. The layers in unit J (Table S2) were described in the field as follows:

Layer 1 (0.07 m): Lenses of reddish brown (Munsell 5YR4/5) fine silty sand with charcoal and rare 1–2 cm limestone clasts. This is a deposit of cultural debris mixed in the sandy fill of the shelter, which was removed in three spits (A–C).

Layer 2 (0.03 m.): Yellowish red (Munsell 5YR 4/6) fine silty sand with rare 1–2 cm limestone clasts, thicker toward the drip line. This must have been carried in by water or wind from the exterior of the shelter, during a time of limited human occupation.

Layer 3 (0.09 m): 3A above was a reddish brown (Munsell 5YR 4/5) silty sand with charcoal, and 3B below was a slightly redder (Munsell 5YR 4/5) silty sand. This is a deposit of cultural debris similar to layer 1, underlain by a deposit with less organic material similar to layers 4 and 5 below.

Layer 4: (0.27 m) Reddish brown (Munsell 5YR 4/5) silty sand with concentrations of charcoal, bone and stone flakes at different levels within the deposit. This was removed in four spits (A–C).

Layer 5: (0.15+ m) Reddish brown (Munsell 5YR 4/5) silty sand and rare 2- to 5-cm rounded limestone clasts, distinctly indurated and harder to excavate than layer 4 above. This layer had occasional fragments of charcoal, bones, and stone flakes at different levels within the deposit, indicating ephemeral occupation. The rounded limestone pebbles noted in layer 5 may have been brought in by human occupants. Three spits (A–C) were fully excavated. A fourth was taken down additional 0.08 m in the west corner, revealing similar sediments, and taking the depth of the unit down to 0.71 m.

In all excavated layers, there were concentrations of fine white material, probably phytoliths, and mollusk shell fragments, largely terrestrial gastropods below layer 3. Given the angle of the rear wall of the cave, we estimate that there are more than 5 m of stratified deposit below. Layers 1–3 are well defined, probably as

a result of ashes and organic material introduced by the later occupants. Layers 4 and 5 have less organic material, perhaps because of a more episodic and ephemeral human occupation. These layers are penetrated by large later termite burrows, which we tried to clean out separately from the surrounding sediment. However, the vertical displacement of radiocarbon dates from layer 5 may indicate that there were other burrows now completely consolidated, which have moved material downward.

Each context was excavated with trowels and sieved in a 1-mm screen. The larger natural rocks were examined for evidence of use and then discarded. Possible chert, bone, ceramic, and charcoal fragments noted during excavation were located in three dimensions and packed separately. Everything remaining was returned to our laboratory in Antsiranana, washed through a 1-mm screen, and dried. In addition, samples from the general excavation of layers 4 and 5 were cleaned in a bath of 10% (vol/vol) HCl for 1 h or more. Everything remaining was dried and sorted under magnification. Samples from the flotation heavy fractions are being cleaned in a 5% (vol/vol) solution of formic acid buffered with calcium phosphate to protect the bone, a procedure developed by Ivy Rutzky of the American Museum of Natural History, New York, NY (24) and tested on our samples by William Sanders of the University of Michigan Museum of Paleontology, Ann Arbor, MI. As at Ambohiposa, the procedure of washing the screened debris and sorting it under magnification yielded not only more bones, but also very small stone artifacts.

Flaked Stone Assemblage from Lakaton'i Anja. Flaked stone items recovered primarily from our washing and sorting procedure are very small, a majority from a range of cryptocrystalline silicates, which we term "chert." In the field notes, we originally termed the coarse flakes "quartzite" and the fine flakes "chert," but the discovery of a stone source 2.5 km to the west near Betahitra indicates they are all chert. The chert items can be opaque and tan or reddish in color. The few unmodified pieces are less than 2 cm in length. In addition, there are a limited number of crystal quartz tools and shatter, predominantly from layers 4 and 5.

Illustrations of flaked stone artifacts are presented in Fig. 4. The stratigraphic distribution of stone items in layers 1B to 5C that provide evidence of human activities in Lakaton'i Anja is presented in Table S2. We note that: (i) Chunks or shatter fragments of raw material are rare in comparison with Ambohiposa, indicating little bipolar core working. (ii) Flakes of a coarse brown chert, found as tabular fragments in gravels in the Betahitra valley, are most plausibly interpreted—given the clear bulbs of percussion and platforms—as consequences of the flaking of tabular chert pieces to make small flakes for cutting tasks or to prepare small stone tools (Fig. 4A–C). No chert cores or core fragments, however, were found. (iii) The weathered reddish sediment of layers 3A, 4, and 5 contain varying amount of small and large chert flakes by weight per unit volume (*Rightmost* column of Table S2). There appear to be concentrations of flakes in spits 4A, 4C, 5A, and 5C. Fine reddish chert in the form of small flakes and tools are found from spits 3B to 5C, but are concentrated in 5A. The source of this stone is unknown. The fine translucent white or tan chert, agate, and obsidian found in Ambohiposa are not attested here.

The formal tools are similar to those from Ambohiposa. Small blades struck from both coarse and fine chert blade cores, are in some cases used (Fig. 4D and F) and one has systematic edge retouch (Fig. 4E). A somewhat larger blade of clear crystal quartz has basal and marginal retouch probably to facilitate hafting (Fig. 4G); the tip has been broken off, but it is likely that that was a pointed projectile tip. Crescentic flakes, also possible projectile elements, are represented by a small example of fine chert (Fig. 4H) and a large example on calcareous chert with

backing and some edge retouch (Fig. 4I). A trapezoidal flake of fine chert (Fig. 4J) made from a blade segment, also a possible projectile element, has a retouched base and utilization on the transverse cutting edge.

The more organic brownish sediments of layers 1 and 3 contain significant densities of coarse chert flakes. Because these layers contain ceramics from the 11th to 14th centuries A.D., when iron was widely smelted and used, it is tempting to suggest that these are extrusive from lower layers. However, if this were true we would expect retouched tools and items of fine red chert and quartz in these later levels as well. None were found, and it is more reasonable to infer that the people who camped in Lakaton'i Anja during the 11th to 14th centuries continued to use locally available coarse chert to make expedient implements for cutting.

As at Ambohiposa, this is a small sample of tiny items. The retouched trapezoidal flake, crescentic flakes, and retouched blades are unquestionably tools. Larger choppers, retouched flakes, or multiply notched tools are not attested. Nevertheless, the fact that the raw materials do not appear to occur near the site and must have been carried in, the evidence of directed blows detaching a series of flakes from cores, and the evidence of retouch or use on some pieces, indicate that this is a stone tool industry created by people.

SI Text S3: Single-Grain Optically Stimulated Luminescence Dating of Sediments from the Cave of Lakaton'i Anja, Madagascar (by Z.J.)

Six sediment samples were submitted for single-grain optically stimulated luminescence (OSL) dating to the Luminescence Dating Laboratory at the University of Wollongong, Wollongong, NSW, Australia. A few radiocarbon (¹⁴C) ages were previously obtained for charcoal fragments from the upper levels (levels 1–3) and three additional accelerator mass spectrometry (AMS) ¹⁴C ages were recently obtained for charcoal from layers 4 and 5. One sample from layer 4A in excavation unit K resulted in a calibrated age of sixth to seventh centuries A.D., similar to a conventional calibrated ¹⁴C age obtained during the 1980s of late third to sixth centuries A.D. Two pieces of charcoal from layer 5A in excavation unit J, however, resulted in calibrated ¹⁴C ages of 10th to 13th centuries A.D., similar to ages obtained in layers 1–3, indicating disturbances in the excavated sediments and the downward percolation of charcoal from the upper levels into the underlying levels.

To investigate the burial ages and stratigraphic integrity of the archaeological deposits at the Cave of Lakaton'i Anja, we measured between 2,800 and 3,000 individual grains from each of the six samples collected.

Sample Collection. Six sediment samples were collected for OSL dating from two excavation units, J and K, and from approximately the same layers in each of the units. The stratigraphic positions and the depths below the current surface of all of the samples are provided in Table S3. The samples were collected by H.T.W., who hammered black plastic tubes, each about 5 cm in diameter and 15 cm long, into the cleaned section face at every chosen sample location. The sampling objective was to collect samples from approximately equivalent levels in both excavation units to facilitate cross-checking.

Sample Preparation. In the OSL Dating Laboratory at the University of Wollongong, the sample tubes were opened under dim red light. Sediment at both ends of each tube was discarded (as it would have contained grains exposed to sunlight at the time of sample collection), and quartz grains were then extracted from the light-safe portions using standard preparation procedures (25, 26). First, carbonates were dissolved in 10% (vol/vol) hydrochloric acid and then organic matter was oxidized in 30% (vol/vol)

hydrogen peroxide solution. The remaining sample was dried and then sieved to isolate grains of 180–212 μm in diameter, and feldspar, quartz, and heavy minerals were separated by density separation using sodium polytungstate solutions of 2.58-, 2.62-, and 2.70-specific gravities, respectively. The separated quartz grains were etched with 48% (vol/vol) hydrofluoric acid for 40 min to remove the α -irradiated rind of each quartz grain and to destroy any remaining feldspars, and then rinsed in hydrochloric acid to remove any precipitated fluorides, dried, and sieved again; grains retained on the 180- μm -diameter mesh were used for dating.

OSL Measurements. OSL measurements were made on individual grains of quartz. We preferred measurement of individual grains over the more conventional multigrain approach because there was clear evidence in the field for termite nests that may have caused some mixing of the sediments. Single-grain dating should allow us to determine whether this was indeed a problem and provide us with a more realistic chance to untangle what part of the sediments are most intact and represents the sediment depositional and “target” event of interest (e.g., ref. 27); this would be the event closest related to the occupation of that layer. The 180- to 212- μm -diameter grains were as a result measured individually using standard single-grain discs (300 μm in diameter and 300 μm deep) (28).

All measurements were made in an identical manner and with the same equipment, using the single-aliquot regenerative-dose (SAR) procedure described elsewhere (29). The SAR procedure involves measuring the OSL signals from the natural (burial) dose and from a series of regenerative doses (given in the laboratory by means of a calibrated $^{90}\text{Sr}/^{90}\text{Y}$ β -source), each of which was preheated at 180 °C for 10 s before optical stimulation by an intense, green (532 nm) laser beam for 2 s at 125 °C. The resulting UV OSL emissions were detected by an Electron Tubes 9235QA photomultiplier tube fitted with Hoya U-340 filters. A fixed test dose (~ 10 Gy, preheated at 180 °C for 5 s) was given after each natural and regenerative dose, and the induced OSL signals were used to correct for any sensitivity changes during the SAR sequence. A duplicate regenerative dose was included in the procedure, to check on the adequacy of this sensitivity correction. As a check on possible contamination of the etched quartz grains by feldspar inclusions, we also applied the OSL IR depletion-ratio test (30) to each grain at the end of the SAR sequence, using an infrared exposure of 40 s at 50 °C.

The equivalent dose (D_e) values were estimated from the first 0.22 s of OSL decay, with the mean count recorded over the last 0.3 s being subtracted as background. The dose–response data were fitted using a linear or saturating exponential function, and the sensitivity-corrected natural OSL signal was projected on to the fitted dose–response curve to obtain the D_e by interpolation. The uncertainty on this estimate (from photon counting statistics, curve-fitting uncertainties, and an allowance of 2% per OSL measurement for instrument irreproducibility) was determined by Monte Carlo simulation, using the procedures described by Duller (31) and implemented in Analyst v3.24. The final age uncertainty includes a further 2% (added in quadrature) to allow for any bias in the β -source calibration. The $^{90}\text{Sr}/^{90}\text{Y}$ beta source was calibrated using a range of known γ -irradiated quartz standards for both multigrain aliquots and individual grain positions. Spatial variations in β -dose rate for individual grain positions were taken into account, based on measurements made using the same γ -irradiated quartz standards (e.g., ref. 32).

Aberrant grains were rejected using the quality-assurance criteria described and tested previously (33). Table S4 provides the details for all samples and the reasons for why single grains were rejected, respectively.

Under these experimental conditions, and using these quality-assurance criteria, we recovered correct dose estimates for single

grains of quartz from sample ANJA_J_5B/C that had first been bleached with natural sunlight for 4 d and then given a known dose (15 Gy) in the laboratory. The weighted mean ratio of measured to given dose (0.97 ± 0.05 , $n = 14$) is statistically consistent with unity, which shows that the chosen SAR procedures can accurately recover a known dose under controlled conditions. An overdispersion (OD) value of 5% was obtained for this dose recovery dataset. Overdispersion refers to the relative spread in the dose distribution above and beyond that associated with the measurement uncertainties of individual grains, and was calculated using the Central Age Model (34). If all of the scatter were because of measurement error alone, then the OD value would be zero.

Environmental Dose-Rate Measurements. The environmental dose rate is mainly because of β - and γ -radiation from the decay of ^{238}U , ^{235}U , ^{232}Th (and their daughter products), and ^{40}K in the deposits surrounding the dated grains. β -Dose rates were measured directly by low-level β -counting of dried, homogenized, and powdered sediment samples in the laboratory, using a GM-25-5 multicounter system (35). Allowance was made for the effect of grain size and hydrofluoric acid etching on the β -dose rate, and a systematic uncertainty of 3% was included in the SE to the β -dose rate. To obtain an estimate of the γ -dose rate for the samples, the same dried, homogenized, and powdered sediment samples used for GM-25-5, β -counting was measured using thick source α -counting (TSAC) to obtain estimates of uranium (U) and thorium (Th). Combining the results obtained from GM-25-5 β -counting and TSAC, an estimate of potassium (K) can be derived by subtraction. The estimates of U, Th, and K, so obtained, were then converted to γ -dose rates using the conversion factors of Adamiec and Aitken (36). This is not the preferred way of estimating the γ -dose rate. A superior way would be to estimate this directly in the field using a γ -spectrometer, which would take into account any homogeneity in the ~ 30 - to 40-cm sphere surrounding the sediment sample. However, we do not believe that this approach will lead to significant error in the age determination.

An assumed effective dose rate of 0.032 Gy/ka was included for α -emitters inside the quartz grains. This value captures (at 2σ) the range of values (0.01–0.05 Gy/ka) measured previously for sedimentary quartz grains from Australia and Africa (37–39). The cosmic-ray dose rates were estimated following Prescott and Hutton (40), taking into account the geomagnetic latitude (6.5°) and altitude (~ 110 m) of the Cave of Lakaton'i Anja, as well as the thickness and density of sediment (variable) and limestone shielding each sample (averaged over the full period of burial). We also allowed for the configuration of the cave by making a correction for the $\cos^2\Phi$ zenith angular distribution of cosmic rays (41). We assigned a relative uncertainty of 10% to account for the systematic uncertainty in the primary cosmic-ray intensity (40). The β -, γ -, and cosmic-ray dose rates were calculated for long-term water contents. We used the current measured field values as representative and assigned a relative uncertainty of $\pm 25\%$ (at 1σ) to accommodate any likely variations over the burial period (Table S5).

Equivalent Dose Results. Of the 17,600 individual grains measured, only 679 grains (3.9% of the total number measured) were used for final D_e determination. Reasons for rejecting individual grains are provided in Table S4. Most grains (86.9% of the total number measured) were rejected because they were too dim following a laboratory dose (T_N signal $< 3 \times \text{BG}$ or T_N error $> 30\%$). These are some of the dimmest samples measured in our laboratory and required measurement of at least three-times the number of grains usually needed. Those grains that were accepted, however, had decay curves and dose–response curves typical of quartz grains dominated by the most light-sensitive

“fast”-component, providing confidence in the accuracy of the resulting D_e estimates. The D_e values for all of the accepted grains are displayed as radial plots in Fig. S3 for each of the samples. In such plots, the most precise estimates fall to the right and the least precise to the left. If these independent estimates are consistent with statistical expectations, then 95% of the points should scatter within a band of width ± 2 units projecting from the left-hand (standardized estimate) axis to any chosen D_e value on the right-hand, radial axis. Thus, the radial plots provide simultaneous information about the spread, precision, and statistical consistency of the D_e values (42). It is immediately apparent from these plots that, for each of the samples, the D_e estimates are spread too widely to fall within any single band of ± 2 units. This finding is also reflected in the D_e OD values (Table S5), which range from $41 \pm 4\%$ (ANJA_J_5B/C) to $72 \pm 7\%$ (ANJA_K_4A), and are greater than the 5% OD obtained for sample ANJA_J_5B/C under controlled laboratory conditions in a dose-recovery test. The range of OD values for the samples from the Cave at Lakaton'i Anja suggests significant contamination.

To further investigate the spread in D_e values and the possible cause of the significant contamination suggested by the degree of OD, we investigated the appearance of the radial plots shown in Fig. S3. Jacobs and Roberts (27) have reviewed explanations of the different general types of radial plot shapes that can be expected from typical processes that affect D_e distributions. What was striking about the radial plots for the samples from the Cave of Lakaton'i Anja was that each of the D_e distributions for grains from each of the samples visually appeared to consist of two to three discrete D_e components. This finding can be explained by the mixing together of grains from two to three sedimentary units with discrete, and significantly different, ages, and is different from mixing that would result from long-term continuous turnover of sediments as might be the case for some soil-forming processes or biological activity. The latter would result in a continuum of D_e values from zero to some upper value, and any stratigraphic evidence would also be obliterated.

We applied the finite mixture model (FMM) to these single-grain datasets to establish the scale of mixing at the Cave of Lakaton'i Anja to further gain insights into the integrity of the sedimentary deposits, and by association, the artifacts. We use the FMM to statistically identify the number of discrete D_e components in each single-grain dataset, estimate the proportion of grains in each component, and determine the weighted mean D_e value and SE of each dose component. The results are summarized in Table S6; worked examples of this procedure have been provided in Jacobs et al. (29, 43). Three fitted components were sufficient to explain the spread in single-grain D_e values for all but one of the samples when OD values of between 15% and 20% were applied to each component. Sample ANJA_J_2/3A was best explained by two fitted components and 15% OD. As the exact value of OD of each dose component is not known, we determined the optimum OD value for each sample independently from a range of reasonable alternatives using maximum log-likelihood and the Bayes Information Criterion (44). From an archaeological standpoint, the most important feature to note is that the vast majority of grains in each sample belong to a single D_e population. For five of the six samples more than two-thirds of the grains in each sample formed a single D_e population. It was only sample ANJA_K_4A that had slightly fewer (~60%) grains forming part of the main D_e population. It is highly likely, therefore, that the artifacts excavated from these layers are contemporaneous with these grains—which form the bulk of the deposit—and were not incorporated at a later date. The one or two minor D_e components, some represented by only 5–8% of the grains (Table S4) and shown as solid gray lines drawn on each of the radial plots in Fig. S3, had D_e values that were both smaller (younger) or

higher (older), suggesting the introduction of these grains into the bulk sediment by small-scale upward and downward movement of grains.

So, what may have caused the scatter observed in the D_e distributions for the samples from the Cave of Lakaton'i Anja? During excavation of the sediments, there was evidence for termite burrows, and it is likely that the sample tubes may have penetrated some of the termite burrows. No systematic study has ever been conducted to explicitly determine the effect of termite burrows on sediment movement and OSL dating, and this would be a worthwhile study to do. However, although we have confirmed the presence of some mixing because of termite activity, we have also shown that the greatest proportion of grains in each sample are in primary context and, thus, accurate ages can be estimated for the associated artifacts from the host single-grain D_e populations.

Environmental Dose-Rate Results. The β -, γ -, and cosmic-ray dose rates were calculated for long-term water contents represented by the measured field values (of 9–17%) and were assigned uncertainties sufficient to accommodate any likely variations over the burial period (Table S5). The total dose rates for the six samples dated in this study show only a modest amount of variation, ranging between 2.34 ± 0.17 and 2.56 ± 0.19 Gy/ka. There is no obvious pattern of variation with depth (Table S5), but the dose rates for samples collected from excavation unit K, however, seems to be systematically higher than those in excavation unit J, but by only a small margin, too small to explain significant differences in age between samples collected from similar layers.

OSL Ages. The final ages for all six samples are listed in Table S5, together with the supporting D_e and dose-rate estimates. Uncertainties on the ages are given at 1σ (SEM) and were derived by combining, in quadrature, all known and estimated sources of random and systematic error. For the sample D_e , the random error was obtained from the model used to determine the weighted mean (i.e., FMM), and a systematic error (of 2%) was included for any possible bias associated with calibration of the laboratory β -source. The total uncertainty on each dose rate was obtained as the quadratic sum of all random (measurement) errors and the systematic errors associated with estimation of the β - and cosmic-ray dose rates. The OSL ages for the six samples are in correct stratigraphic order within each excavation unit, but also between the two excavation units when taking into consideration the layer and sublevel assignments. The ages range from ca. 930 y (11th century A.D.) at the top of excavation unit J (layer 2/3A) to ca. 4,300 y at the base of excavation unit J (layer 5B/C). In excavation unit K, the ages range from ca. 1,330 y (seventh century A.D.) at the top (layer 3A) to 3,470 y at the base (layer 5A/B). The ages for layer 3 in excavation unit J is consistent with ^{14}C ages from this layer, but the age for layer 3A in excavation unit K is more consistent with the ^{14}C ages obtained for the underlying layer 4. However, this sample is the most mixed of all measured and 32.5% of the grains in this sample resulted in an age of ~600 y (14th century A.D.) that is consistent with the ^{14}C ages. However, our single-grain OSL ages for layer 4 are not compatible with the ^{14}C ages obtained for layer 4, and we suggest that the charcoal that have been measured for these layers may, in fact, have been intrusive, as was the case for those collected from layer 5. We can postulate that if it is indeed termites that caused the mixing, then they would likely move charcoal along, as this would be a source of moisture; moisture management is the prime reason for termite burrowing.

In both excavation units, the sedimentation appears not to have been continuous throughout the period, which is also supported by the discrete nature of the D_e components, as can be seen in the radial plots (Fig. S3) and verified by the FMM (Table S5). Overall, there is good internal stratigraphic coherence among

the OSL ages from similar layers and different excavation units, but it has to be borne in mind that because of the small-scale mixing, untangling of the different D_e components may lead to some additional uncertainty.

SI Text S4: A Note on Ceramics from Lakaton'i Anja (by C.R. and H.T.W.)

Introduction. Both the excavations in the 1980s and the excavations of 2012 produced a range of pottery fragments in the uppermost layers. In 2012, ceramics found below layer 2 were in termite burrows. The earlier visitors to Lakaton'i Anja, whose remains were found in layers 3A to 5C, may have used pottery, but we have little evidence of this. Locally manufactured ceramics occur in layers 1 and 2 in low densities compared with contemporary village sites. The many plain body fragments require further study, but the rims represent familiar ceramics known from other sites in Madagascar.

Local Ceramics. Locally manufactured ceramic rims manifest technology and designs well-known from other sites in northern Madagascar, particularly from the 11th to 15th century port town of Mahilaka, 190 km southwest of Andavakoera (45, 46). All examples have sandy bodies with fine sand inclusions constituting up to 20% of the clay body, which may be natural constituents of the potting clay. Some also have angular quartz fragments, which must be deliberate inclusions. Both oxidized and reduced sherds occur. Diagnostic rims of three small vessels representing different forms were recovered from layer 1 of unit K, and these can be supplemented with rims from the 1980s excavations. One—a restricted small jar with out-curved rim—is decorated with incised zigzags made with a blunt tool on its out-curved neck (Fig. S4E). A similar small jar from the earlier excavations has a wavy combed decoration on its neck (Fig. S4D), and another has rows of small punctuates (Fig. S4F). Isolated sherds, perhaps from such jars, have oblique fine incised lines made with something like an iron knife (Fig. S4I). The first two design formats have parallels from roughly A.D. 1200–1500 at Mahilaka. Another form is a small restricted bowl with an undecorated body. The example from unit K has a thickened or beaded rim (Fig. S4G), and those from the earlier excavations have simple rounded lips (Fig. S4B and H). From unit K there is a unique small open bowl with oxidized body and burnished red-brown slip, decorated with three rows of grass impressions inside the rim (Fig. S4A). This finding has close parallels from the 11th–14th century Maliovola phase of the far Southeast Coast (figure 3 I and L–R in ref. 47). The closest known example is from the 12th–14th century Fiekena phase of the central highlands (figure A151, *Lower Middle*, in ref. 48) 730 km south of Andavakoera. Attested only in the earlier excavations is a heavy spherical vessel (Fig. S4C), a cooking vessel common in all early ceramic assemblages throughout the island. Absent at Lakaton'i Anja are large bowls or basins, often slipped with a red iron oxide coating during this period, and rare are large restricted jars either spherical or with out-turned necks. Only one vessel has a mouth greater than 20 cm in diameter.

There is evidence of carved stone vessels. In 2012 only a small fragment of chlorite schist was found, but from the earlier excavations there is a vessel fragment (Fig. S4J). It is from the lower body of a deep basin. Such sherds are often worked into other items, such as net weights or spindle whorls; the occurrence of one sherd at Anja does not necessarily mean that stone vessels were used there. The ridge on the sherd suggests it was finished on a large lathe, a technique documented from the 10th to the 16th centuries. The nearest chlorite schist report known to us is near the Bay of Andravina, 90 km to the southeast of Andavakoera.

Imported Ceramics. Most of the fragments of pottery made elsewhere and imported to Madagascar are from glazed *sgraffiato* bowls made in the area of the Persian Gulf between A.D. 1100 and 1300. Most have a yellow-to-brown glaze on a fine light brown to pink body. Rim sherds and well preserved designs, which would allow a more precise dating (see, for example, ref. 49), are not present. One sherd, not large enough to exhibit any incision, has a green glaze, and may date as late as A.D. 1500.

In addition to imports of Near Eastern origin, there is a tiny fragment of the distinctive ring base of small bowl of clear-glazed white porcelain, made in southern China during the Song Dynasty or slightly later (*ca.* A.D. 960–1300). Song and Liao bowls of the same form from northern China are of stoneware rather than porcelain and later white-ware porcelain bowls have thinner ring bases, so we are reasonably confident of the ascription. This complements the date based on the *sgraffiato*.

Comment. Although the ceramics, both local and imported, are useful in establishing the date of layer 1 to roughly A.D. 1200–1500, they also raise other more interesting questions.

First, why does Lakaton'i Anja have only a limited range of the pottery found on contemporary village sites, and a predominance of small vessels? One possible explanation is that only small groups visited the site and they prepared and consumed small portions of food. Another possibility is that special activities, such as possession ceremonies or initiation rituals demanding special foods, were undertaken in the cave. Analysis of residues on the sherds might help to evaluate these possibilities.

Second, why would a group with such a limited range of containers (and other imperishable items as well) used and break a number of presumably rare vessels imported from as far away as China and Mesopotamia? One possible explanation is that the cave was visited by people from foreign ships, whose crews routinely used such ceramics, a possibility suggested after the earlier excavations (50). The most obvious way to evaluate this idea would be to study a shipwreck of this period on the coast of Madagascar.

SI Text S5: Beads from Lakaton'i Anja 2011 Excavation Season (by G.O.K.)

Six glass beads from the 2011 excavation season at Lakaton'i Anja, Madagascar (Fig. S5) were brought to the United States for research and analysis. These small dark brown, aqua, and red glass beads are typical of the varieties found at many sites in Madagascar and Southern Africa, which are generally believed by scholars to have been imported via the Indian Ocean trade, which was active from at least the first century C.E., but for which there is evidence in Madagascar after 700 C.E. (51).

Considering both the dating of the layers from which these beads come (circa 1200–1400 C.E.) and their appearance, the six glass beads recovered from excavations at Lakaton'i Anja clearly belong to a broad category called “trade wind beads” by Van Der Sleen (52), or “Indo-Pacific Monochrome Drawn Beads” by Francis (53). This class of beads are made by the technique of tube-drawing: gathering a lump of molten glass on the end of a tapering pipe (*lada* in contemporary glass-bead making), which is then drawn out by two people, pulling the glass into a long and thin tube between the *lada* and another iron rod with a hook on the end. This hollow glass tube, once cooled, is then cut into short lengths of a few millimeters. These tube segments are then reheated and rolled to round the sharp edges (53). These beads most likely come from India, although exact sources and sites have only been established in a few cases (51, 54, 55).

Previous research on beads from the contemporary sites of Mahilaka and Sandrakatsy in Madagascar has indicated that there were two glass-bead types present in Madagascar during this period (45, 55, 56). Using laser ablation-inductively coupled plasma-mass spectrometry, researchers found that half of the

beads from Mahilaka belong to the category of mineral-soda-Alumina glass identified as m-Na-Al 2, which used mineral-based soda as a flux, and the other half were made with a plant-ash soda (51, 55, 57). Dussubieux et al. (54) suggest that the 15 m-Na-Al glass beads analyzed from Mahilaka are compositionally most similar to beads from the port site of Chaul on the west coast of India (58).

Although compositional analysis has not been undertaken on the beads from Lakaton'i Anja, tentative identifications can be made based on comparison of color, shape, size, and opacity/diaphaneity, between these beads and the known glass types described and illustrated in publications, (e.g., refs. 51, 54, and 58). The red beads are most distinctively of Indian manufacture, probably of the type designated as m-Na-Al 2 by Dussubieux et al. (54). The dark brown/black beads are less easily identified, although their technique of manufacture is the same. Dussubieux et al. (54) suggest that the m-Na-Al beads may have been produced in India primarily for export to eastern Africa (and presumably also Madagascar), based on their distributions and numbers of beads found at various archaeological sites in these two regions.

The aqua/blue-green glass bead can be tentatively identified as belonging to the Zimbabwe series identified by Robertshaw et al. (51). This is a particular type of bead for which the source is probably in South Asia, although from an unknown production center. The chemistry of the Zimbabwe series is based on plant-ash flux rather than a mineral soda, and is datable to between 1300 and 1430 C.E., and found in large numbers at Great Zimbabwe and related sites (51). Several beads from the contemporaneous site of Mahilaka have also been identified as belonging to the Zimbabwe series (51, 55). Alternatively, this blue-green bead could come from the slightly later Khami series, dated to the early 15th century. The Khami series beads appear similar to the Zimbabwe series, and the assemblages have roughly similar proportions of blue, blue-green, yellow, black, brownish-red, and orange glass beads; the Khami series is the only series of

beads in Madagascar or Southern Africa with opaque white glass beads. Chemically the Zimbabwe series and the Khami series are radically different, as the Khami series represents a return to the use of mineral soda rather than plant ash, common before the Zimbabwe series (59). Direct observation of color, shape, size, and other attributes allows us to formulate hypotheses that need to be tested with compositional analysis.

Chronologically, therefore, according to Robertshaw et al. (51), the red Indo-Pacific beads should belong to older levels from 1000–1250 C.E., and the blue/green (probable) Zimbabwe series bead should belong to somewhat later levels, 1300–1430 C.E., although older beads can be curated, and mixing because of postdepositional processes can occur.

SI Text S6: Geological Observations on Sediment Samples from Ambohiposa, Madagascar (by F.B.)

Four loose sediment samples from 2007 sounding at the rock shelter of Ambohiposa, termed the “central unit,” were submitted to our laboratory. These samples are from layers termed layers 3, 4, 5, and 6 in this report. The analyses were conducted by F.B. with advice from the Director of the laboratory, Paul Goldberg, at Boston University, Boston, MA.

The samples were air-dried, homogenized, and analyzed by Fourier transform infrared spectroscopy (FT-IR) using a Thermo-Nicolet Nexus 470 spectrometer. Representative FT-IR spectra were obtained by grinding a few tens of micrograms of sample using an agate mortar and pestle. About 0.1 mg or less of the sample was mixed with about 80 mg of KBr (IR-grade). A 7-mm pellet was made using a hand press (Qwik Handi-Press; Spectra-Tech Industries) without evacuation. The spectra were collected between 4,000 and 400 cm^{-1} at 4- cm^{-1} resolution.

The FT-IR spectra of the four samples from Ambohiposa and Kaolinite standard K-Ga-1b (red pattern) are given in Fig. S6. The four Madagascar samples show FT-IR patterns characteristic of kaolinite (538, 915, 1,030, 3,619, and 3,695 cm^{-1}) and quartz (at 1,080, 800, 780, and 695 cm^{-1}).

- Vérin P (1986) *The History of Civilisation in North Madagascar* (Balkema, Rotterdam, Boston).
- Battistini R (1965) Le Quaternaire littoral de l'extrême nord de Madagascar. *Bulletin de l'Association française pour l'étude du quaternaire* 2(2):133–144.
- Battistini R (1977) Ages absolus $\text{Th}^{230}/\text{U}^{234}$ de dépôts marins Pleistocènes à Madagascar et dans les îles voisines. *Rev Géog* 23:73–86.
- Donque G (1975) *Contribution Géographique à l'étude des Climats de Madagascar* (Imprimeries des Arts Graphiques, Antananarivo).
- Ranaivonasy J, Andrianjaka N (2003) Aires prioritaires pour la conservation des plantes. *Ravintsara* 15(5):14–15.
- Randrianarisoa PM, Rasamison AA, Rakotozafy L (1999) Les lémuriens de la région de Daraina: Forêt de Bekaraoka et forêt de Sahaka. *Lemur News* 4:19–21.
- Raheriarisena M, Goodman S (2006) *Inventaires de la Faune et de la Flore du Nord de Madagascar*, eds Goodman S, Wilimé L (Ministère de l'Education et de la Recherche Scientifique, Antananarivo), pp 175–230.
- Safford RJ, ed (2000) *Etude Environnementale et écologique du Lac Sahaka, Madagascar* (Royal Holloway Institute for Environmental Research, London).
- Levat D (1912) *Richesses Minérales de Madagascar* (H. Dunod and E. Pinat, Paris).
- White JP, Thomas DH (1972) *What Mean These Stones?* (Methuen, The Hague).
- Binford LR, Quimby GI (1963) Indian sites and chipped stone materials in the northern Lake Michigan area. *Fieldiana (Anthropology)* 36(12):277–307.
- Shott MJ (1999) On bipolar reduction and splintered pieces. *N Amer Arch* 20(3): 217–238.
- Rossi G (1980) *L'Extrême-nord de Madagascar* (Edisud, Aix-en-Provence).
- Mavume AF, Rydberg L, Rouault M, Lutjeharms JRE (2009) Climatology and landfall of tropical cyclones in the south-west Indian Ocean. *Western Indian Ocean Journal of Marine Sciences* 8(1):15–36.
- Dewar RE, Richard AF (2007) Evolution in the hypervariable environment of Madagascar. *Proc Natl Acad Sci USA* 104(34):13723–13727.
- Burney DA (1987) Late quaternary stratigraphic charcoal records from Madagascar. *Quat Res* 28(2):274–280.
- Godfrey LR, Jungers WL, Simons EL, Chatrath PS, Rakotosamimanana B (1996) in *New Directions in Lemur Studies*, eds Rakotosamimanana B, Rasamimanana H, Ganzhorn JU, Goodman SM (Kluwer, Plenum, New York), pp 19–53.
- Simons EL, et al. (1995) AMS ^{14}C dates for extinct lemurs from caves in the Ankarana Massif, Northern Madagascar. *Quat Res* 43(2):249–254.
- Ganzhorn JU, Malcomer S, Andrianantoanina O, Goodman SM (1997) Habitat characteristics and lemur species richness in Madagascar. *Biotropica* 29(3):331–343.
- Goodman SM, Ganzhorn JU, Olson LE, Soarimalala V (1996) Patterns of elevational distribution of birds and small mammals in the humid forests of Montagne d'Ambre, Madagascar. *Ecotropica* 2:87–98.
- Baum DA (1995) A systematic revision of *Adansonia* (Bombacaceae). *Ann Missouri Bot Gdns* 82(3):440–471.
- D'Cruze N, et al. (2007) The first comprehensive survey of amphibians and reptiles at Montagne des Français, Madagascar. *Herp Conserv Biol* 2(2):87–99.
- Sabel J, et al. (2009) The conservational status of mammals and avifauna in the Montagne des Français massif, Madagascar. *Mad Conserv Devel* 4(1):44–51.
- Blench R (2007) New palaeogeographical evidence for the settlement of Madagascar. *Azania* 42:69–82.
- Wintle AG (1997) Luminescence dating: Laboratory procedures and protocols. *Radiat Meas* 27(5–6):769–817.
- Aitken MJ (1998) *An Introduction to Optical Dating* (Oxford Univ Press, Oxford).
- Jacobs Z, Roberts RG (2007) Advances in optically stimulated luminescence dating of individual grains of quartz from archeological deposits. *Evol Anthropol* 16(6):210–223.
- Botter-Jensen L, Bulur E, Duller GAT, Murray AS (2000) Advances in luminescence instruments systems. *Radiat Meas* 32(5–6):523–528.
- Jacobs Z, et al. (2008) Ages for the Middle Stone Age of southern Africa: Implications for human behavior and dispersal. *Science* 322(5902):733–735.
- Duller GAT (2003) Distinguishing quartz and feldspar in single grain luminescence measurements. *Radiat Meas* 37(2):161–165.
- Duller GAT (2007) Assessing the error on equivalent dose estimates derived from single aliquot regenerative dose measurements. *Ancient TL* 25:15–24.
- Ballarini M, Wintle AG, Wallinga J (2006) Spatial variation of dose rates from beta sources as measured using single grains. *Ancient TL* 24:1–8.
- Jacobs Z, Duller GAT, Wintle AG (2006) Interpretation of single grain D_e distributions and calculation of D_e . *Radiat Meas* 41(3):264–277.
- Galbraith RF, Roberts RG, Laslett GM, Yoshida H, Olley JM (1999) Optical dating of single grain and multiple grains of quartz from Jimmum rock shelter, northern Australia: Part I, experimental design and statistical models. *Archaeometry* 41(2A): 339–364.
- Botter-Jensen L, Mejdahl V (1988) Assessment of beta dose-rate using a GM multiscaler system. *Nucl Tracks Radiat Meas* 14(1–2):187–191.
- Adamiec G, Aitken MJ (1998) Dose-rate conversion factors: Update. *Ancient TL* 16: 37–49.
- Feathers JK, Miglorini E (2001) Luminescence dating at Katanda—A reassessment. *Quat Sci Rev* 20(5–9):961–966.

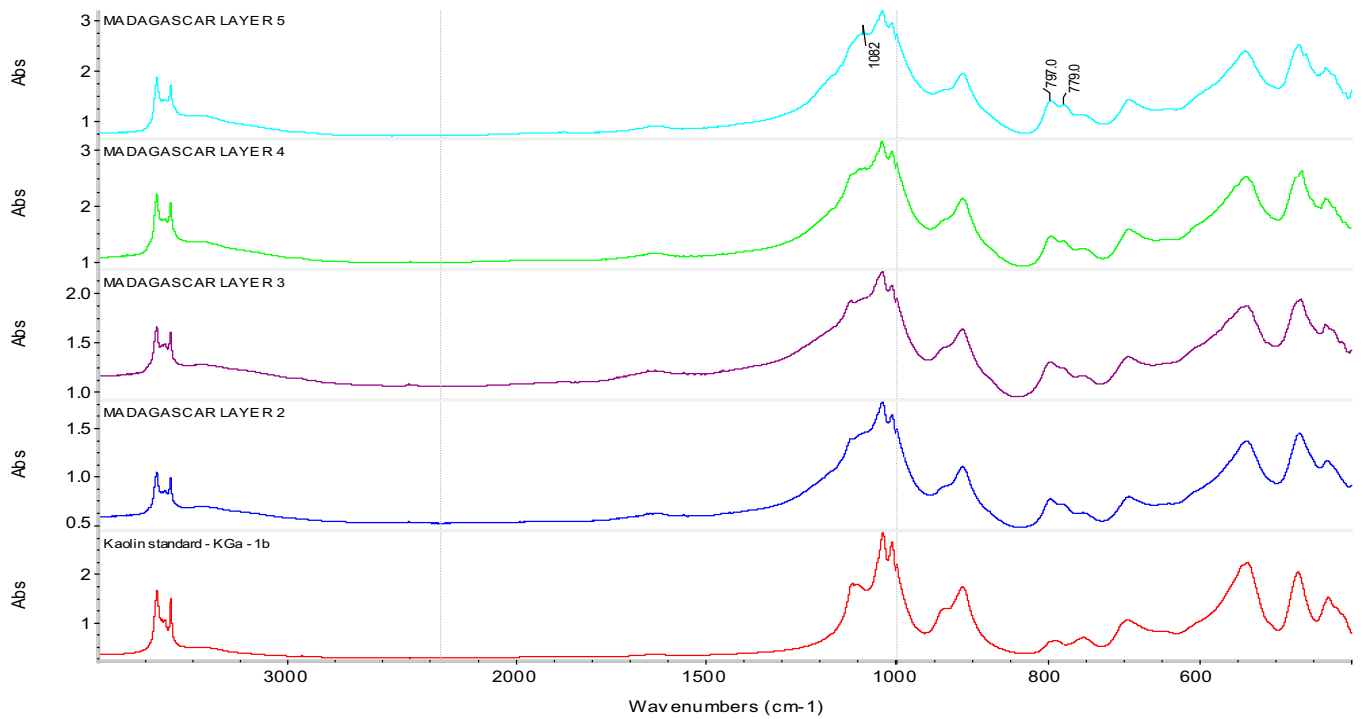


Fig. S6. FT-IR spectra from layers 3–6 at Ambohiposa.

Table S1. Ambohiposa stone tool distribution (south and central units)

Layer	Volume (L)	Observed counts and weights				Counts and weights/liter and mean weights			
		Coarse flakes	Chert shatter	Chert flakes	Obsidian flakes	Coarse flakes	Chert shatter	Chert flakes	Obsidian flakes
3	101	199	238	43	3	1.97	2.36	0.42	
		46.6 g	16.8 g	2.6 g	0.1 g	0.46 g	0.17 g	0.03 g	0.01g
4	99	460	379	46	0	4.65	3.82	0.46	—
		80.7 g	62.8 g	1.7 g	—	0.81 g	0.63 g	0.02 g	—
5	39	145	250	56	4	3.72	6.41	1.43	0.10
		16.0 g	28.2 g	4.3 g	0.7 g	0.41 g	0.72 g	0.11 g	0.02 g
6Up	34	156	142	21	5	4.59	4.17	0.61	0.15
		9.0 g	7.8 g	0.4 g	0.3 g	0.26 g	0.23 g	0.01 g	0.01 g
6Lo	27	145	250	56	4	1.92	1.56	0.11	—
		16.0 g	28.2 g	4.3 g	0.7 g	0.13 g	0.07 g	0.02 g	—
						0.07 g	0.05 g	0.17 g	—

Table S2. Lakaton'i Anja stone tool distribution (unit J)

Layer	Area (m ²)	Volume (L)	Coarse chert flakes				Fine chert flakes		Comment	Total flake weight (g) per 10 L
			Large		Small		No.	g		
			No.	g	No.	g				
1B	0.96	28.8	13	5.1	15	2.1	—	—	2.5	
1C	0.78	22.8	11	9.4	1	—	—	—	4.1	
3A	0.79	31.6	6	6.6	—	—	—	—	2.1	
3B	0.79	49.5	3	3.2	11	0.9	1	0.1	Chlorite schist fragment	0.8
4A	0.77	53.9	21	5.8	30	2.7	—	—	Coarse chert blade*	1.6
4B	0.86	68.8	10	5.0	4	—	—	—	Coarse chert blade*; Crystal blade*	0.7
4C	0.92	46.0	11	6.9	21	0.6	2	0.01	Fine chert crescent*; Fine chert trapeze*	1.6
4D	0.92	64.0	8	4.5	22	1.4	7	0.02	Coarse chert blade	0.9
5A	0.92	46.5	16	15.6	26	2.1	20	0.06	Small crystal splinter; Coarse chert crescent*	3.8
5B	0.99	39.6	4	3.5	26	1.6	—	—	—	1.3
5C	0.99	29.7	16	6.9	42	1.4	1	0.01	Small crystal quartz blade; Small chert chunk	2.8

*The item is illustrated in this paper.

Table S3. Summary of sample locations and depths below surface

Sample	Depth below surface (cm)	Excavation unit	Layer
ANJA_J_2/3A	15	J	2/3A interface
ANJA_K_3A	22	J	3A
ANJA_K_4A	37	K	4A
ANJA_J_4A/B	38	J	4A/B interface
ANJA_K_5A/B	55	K	5A/B interface
ANJA_J_5B/C	59	J	5B/C interface

Table S4. Information on the number of individual grains measured, the number of grains rejected and for what reasons, and the total number of grains for which D_e values were determined

Sample	Grains measured	Reasons for rejection of grains				Total rejected	Total accepted	% used
		A	B	C	D			
ANJA_J_2/3A	2,900	2,509	170	103	1	2,783	117	4.0
ANJA_K_3A	2,900	2,538	158	96	3	2,795	105	3.6
ANJA_K_4A	2,800	2,443	146	93	18	2,700	100	3.6
ANJA_J_4A/B	3,000	2,580	199	102	5	2,886	114	3.8
ANJA_K_5A/B	3,000	2,627	170	92	9	2,898	102	3.4
ANJA_J_5B/C	3,000	2,596	161	96	6	2,859	141	4.7
Total	17,600	15,293	1,004	582	42	16,921	679	3.9

Reasons for rejection are: A, T_N signal < 3 × BG and the error associated with the T_N signal is >30%; B, recycling ratio deviates more than 2σ from unity; C, OSL IR depletion ratio is more than 2σ less than unity; D, L_N/T_N dose not intersect the sensitivity-corrected dose–response curve.

Table S5. Dose rate data, D_e values, and OSL ages for six sediment samples from the Cave of Lakaton'i Anja

Sample name	Moisture content (%)	Dose rates (Gy/ka)			Total dose rate (Gy/ka)	D_e (Gy)	Number of grains	Age model	OD (%)	OSL age (ka)
		β	γ	Cosmic						
Excavation Unit J										
ANJA_J_2/3A	9.1	1.18 ± 0.07	1.07 ± 0.10	0.10 ± 0.01	2.38 ± 0.18	2.21 ± 0.14	117	FMM	55 ± 6	0.93 ± 0.09
ANJA_J_4A/B	10.7	1.18 ± 0.07	1.03 ± 0.08	0.10 ± 0.01	2.34 ± 0.17	6.31 ± 0.26	114	FMM	49 ± 5	2.70 ± 0.23
ANJA_J_5B/C	16.6	1.17 ± 0.08	1.14 ± 0.11	0.10 ± 0.01	2.44 ± 0.20	10.56 ± 0.37	141	FMM	41 ± 4	4.38 ± 0.40
Excavation unit K										
ANJA_K_3A	9.7	0.56 ± 0.04	1.17 ± 0.10	0.10 ± 0.01	2.56 ± 0.19	3.40 ± 0.20	105	FMM	56 ± 6	1.33 ± 0.13
ANJA_K_4A	6.3	0.55 ± 0.04	1.12 ± 0.09	0.10 ± 0.01	2.47 ± 0.18	5.48 ± 0.22	100	FMM	72 ± 7	2.21 ± 0.19
ANJA_K_5A/B	12.9	0.54 ± 0.04	1.18 ± 0.12	0.10 ± 0.01	2.54 ± 0.22	8.82 ± 0.54	102	FMM	58 ± 6	3.47 ± 0.37

The total dose rate includes an allowance of 0.032 ± 0.003 Gy/ka for the internal dose rate.

Table S6. D_e values and the proportion of grains associated with each dose component identified by the FMM

Sample name	OD (%)	Dose component 1		Dose component 2		Dose component 3	
		D_e (Gy)	Proportion (%)	D_e (Gy)	Proportion (%)	D_e (Gy)	Proportion (%)
ANJA_J_2/3A	15	2.21 ± 0.14	70.8	5.32 ± 0.47	29.2	—	—
ANJA_J_4A/B	20	0.70 ± 0.23	4.7	2.48 ± 0.48	8.1	6.31 ± 0.26	87.2
ANJA_J_5B/C	15	1.86 ± 0.43	7.1	5.64 ± 0.61	21.0	10.56 ± 0.37	71.9
ANJA_K_3A	15	1.45 ± 0.13	32.5	3.40 ± 1.99	59.8	8.53 ± 0.13	7.7
ANJA_K_4A	15	0.94 ± 0.23	7.1	5.48 ± 0.22	72.1	18.55 ± 1.33	20.8
ANJA_K_5A/B	20	2.45 ± 0.34	23.7	8.82 ± 0.54	70.8	20.36 ± 7.56	5.5

Table S7. Basic data on glass beads from Lakaton'i Anja 2011 excavation

Number	Provenance	Color description	Munsell Color	Length (mm)	Diameter (mm)
1	Unit K – 1B	Aqua	5G 6/4	2.44	3.70
2	Unit J – 4B	Dark brown	2.5YR 2/2	2.15	3.23
3	Unit J – 1B	Red	7.5R 4/8	3.49	2.25
4	Unit J – 1B	Dark brown	2.5YR 2/2	1.64	2.45
5	Unit J – 1C	Red	10R 4/6	2.70	3.82
6	Unit J – 1C	Red	7.5R 4/6	2.85	2.95